Pinnacles on the surface of the comet 67P/Churyumov-Gerasimenko: regional distribution and morphology

S. S. Krasilnikov,[1,2]⋆ Y. V. Skorov,[2,3] A. T. Basilevsky[1,2] S. F. Hviid[4] U. Mall[2] and H. U. Keller[3]

[1] *Vernadsky Institute of Geochemistry and Analytical Chemistry RAS, Kosygin 19, Moscow, 119334, Russia*
[2] *Max Planck Institute for Solar System Research, Justus-von-Liebig-Weg 3, Göttingen, D-37077, Germany*
[3] *Institute for Geophysics and Extraterrestrial Physics, TU Braunschweig, Braunschweig, D-38106 Germany*
[4] *Institute of Planetary Research, DLR, Rutherfordstrasse 2, Berlin, D-12489 Germany*

Accepted XXX. Received YYY; in original form ZZZ

ABSTRACT

Pinnacles are local topographic promontories of different shapes considered to be formed due to uneven surface erosion. In the case of comets, areal changes in the degree of erosion could be related to inhomogeneities of the nucleus. However, the amount of solar radiation and the thermal gradient is different across the orbit for geomorphological regions, which can result in different erosion and shape for a similar composition among two differently illuminated areas. Therefore, a study of the areal distribution of pinnacles on the nucleus surface and their morphology may help to understand the structure and properties of the nucleus material. We mapped 166 pinnacles on the comet nucleus surface of 67P/Churyumov-Gerasimenko. About a third of them have planimetrically rounded shape (rounded pinnacles) and the rest are planimetrically elongated (local ridges). In the southern hemisphere, number of both round pinnacles and local ridges is larger than in the northern hemisphere. This difference possibly indicates the higher effectiveness of the pinnacles' formation in the southern hemisphere. At the same time the mean values of the measured parameters, including the height, show no statistically reliable difference between the north and south. We found that the maximum height of the pinnacles is about a hundred meters. Suggesting that they have been formed by sublimational erosion, this value allows estimating the minimum thickness of the eroded material and thus the degree of the evolutionary changes of the nucleus. In our future study, we will model pinnacles formation based on the here presented analysis of observations.

Key words: comets: general - comets: individual: 67P/C-G - Kuiper belt: general - Planets and satellites: formation

1 INTRODUCTION

Pinnacles are local promontories of different shapes. The term "pinnacle" is widely used in the Earth's geology (see e.g., Lipar & Webb 2015) and usually is defined as a local positive isolated structure, in a shape of a vertical shaft or spire. It consists of material, more resistant to erosion, than the surrounding surface. In the context of comets, the term "pinnacle" was used for the first time in the description of the nucleus of comet Wild 2 by Brownlee et al. (2004) and later by Basilevsky & Keller (2006) and Cheng et al. (2013). Brownlee et al. (2004) noted that cometary pinnacles have varied shapes including spires and sizes from tens of meters to over a hundred meter in height. They also hypothesized that their formation might be due to an uneven sublimational surface erosion. Therefore, the areal distribution of pinnacles and their sizes and morphologies are possibly indicative of inhomogeneities of a cometary nucleus. Following this work and continuing our previous research (Basilevsky et al. 2017a) we distinguish pinnacles into separate classes of formation on the surface of the cometary nucleus.

It should be noted that cometary surface elevated features are of different scales. The smallest visible on the nucleus consolidated material at high resolution images (tens of centimeters to several meters) are so-called knobs (Bibring et al. 2015; Davidsson et al. 2016; Mottola et al. 2015; El-Maarry et al. 2015b; Basilevsky et al. 2017b). The pinnacles shortly described above refer to medium-sized for-

⋆ E-mail: krasilnikovruss@gmail.com (KSS)

mations. And the large-scale structures are regional ridges described for example in El-Maarry et al. (2015a).

The pinnacles are best recognized near the terminator or the limb (Fig. 1). Bases of pinnacles can be covered by redeposited smooth material and/or boulders possibly leftovers from the erosion of the pinnacles.

On the nucleus of comet 67P/Churyumov-Gerasimenko, pinnacles were first identified by Basilevsky et al. (2017a). In general, their identification is best performed with complementary use of OSIRIS and NavCam images and 3D model of the nucleus. In Basilevsky et al. (2017a), morphometric parameters and the position of the identified pinnacles were determined mainly on the northern hemisphere, because at that time, a statistical analysis for the southern hemisphere was not feasible due to the limited set of observations. Now high-resolution images of both hemispheres as well as a meter-level digital terrain model of the total cometary surface (Preusker et al. 2017) are available (https://imagearchives.esac.esa.int). This allows us to perform a detailed quantitative analysis of the locations of pinnacles and their basic characteristics for the whole nucleus.

2 MEASUREMENTS AND ANALYSES

Our findings in this paper are based on the open access images from the NavCam (Geiger & Barthelemy 2015) and OSIRIS NAC (Keller et al. 2007) cameras. The resolution of the used images is varying and reaches its highest values at about 2 m/pix for the NavCam and 0.04 m/pix for the OSIRIS NAC (Geiger & Barthelemy 2015; Keller et al. 2007). For the spatial and morphometric analysis, the high-resolution shape model SHAP7 of the nucleus with a horizontal resolution of 1 - 1.5 m and a total vertical accuracy of 0.3 m is used (Preusker et al. 2017). Using this shape model, we identify pinnacles starting from about twenty meters in diameter and approximately ten meters in height. For our analysis we use the subdivision of the surface into geomorphological regions following El-Maarry et al. (2015a), El-Maarry et al. (2016), Lee et al. (2016) and Giacomini et al. (2016). For each promontory an ascending number is assigned in the regions listed in alphabetical order (Table A1 in the Supplementary materials).

Using the shape model SHAP7, a metrical analysis (see sketches in Fig. 2) of the identified pinnacles is executed. Due to complex shape of the nucleus surface measuring the basic characteristics of pinnacles is not an easy task and inevitably leads to some voluntarism. The major difficulty arises in determining the pinnacle base because these features are never located on a perfect flat plain. Very often, the curvature of the surrounding region is comparable to the size of the pinnacle itself. Therefore, we use a fairly qualitative approach to determine the position of the base: we look for the contour inflection points, suggesting that it is the change in slope that characterizes the boundaries of the pinnacle base.

Each pinnacle is measured in two planimetric directions: the first cross section (*A'B'C'* in Fig. 2) passes through two points of inflection (*A'* and *B'*) that define the baseline d and apex (*C'*), and the second cross section cuts the pinnacle through the bigger baseline (*D*) (i.e., pinnacle lengthwise) and apex. Besides a smaller pinnacles size *d'* is measured at mid-height *h/2* of the pinnacle (Fig. 2). Inclination of pinnacles to local gravity is measured as differences between line *h* and plumb line *g* (tilt angle - Φ). The slope angle (α and β) is defined as shown in Fig. 2: this is the angle between the averaged tangent line of slope and the smaller planimetric direction baseline *d*. The results of the measurements and their statistical analysis are presented in Table 1 and Table A1.

2.1 Pinnacle types

A total 166 pinnacles are identified. To perform a quantitative analysis, we divide them into two sub-classes: (1) pinnacles having planimetrically equidimensional shape - "rounded pinnacles", and (2) pinnacles having planimetrically elongated shape, so-called "local ridges". As a separating characteristic, we use the ratio of d/D: for the first type of formations $d/D<0.7$, for the second ones $d/D>0.7$. The chosen value is arbitrary and based on a simple perception of the form by eye. We assume that formations with $d/D>0.7$ are close to the rounded form. The main results of our statistical analysis presented below are not sensitive to insignificant changes of this parameter. To prove that, we performed additional calculations for the specific value in the range of 0.6 - 0.8. All our main conclusions are still valid for considered cases.

In lateral views, pinnacles are typically asymmetric and sometime even have negative angles of part of their slopes. The slope inclination is calculated using the angle between the slope and the smaller baseline in the base of the pinnacle. The mean slope inclination for rounded pinnacles is about 57(±22 of standard deviation) and for local ridges 64(±19). The mean deviation of pinnacles from the plumb line (*g*), on the Fig. 2 is ~34 with standard deviation ±20and statistical dispersion near 90. Significant inclination and a large dispersion indicate a rather weak correlation between the pinnacle vertical orientation and the local gravity vector. Cliffs and overhangs, considered in the work of Attree et al. (2018), are found on approximately 0.52% of all shape model (SHAP7) facets, having slopes of 90 - 100 and approximately 0.25% showing slopes >100.

In Fig. 4, we show a map of locations of the identified and analyzed objects. Statistical analysis shows that a latitudinal distribution of promontories is not uniform: the main part of rounded pinnacles is concentrated in the equatorial and sub equatorial zone, whereas local ridges have a more homogeneous distribution, but a concentration in the low latitudes is also noticeable (Fig. 3). This could be due to the larger surface area in the lower latitudes comparing to the higher ones.

It is seen from the Table 1 that morphometric parameters of the pinnacles are quite variable. Using the Student's t-test for the probability level 95% and comparing the considered parameters for the northern and southern hemisphere and the total surface one can find that statistically significant difference is observed only for the elongation of ridges of the north and south while for all other parameters the differences between north, south and total surface are insignificant. Below we shortly describe the observational results for rounded pinnacles and local ridges separately (Fig. 5, 6 7 and 8).

Rounded pinnacles

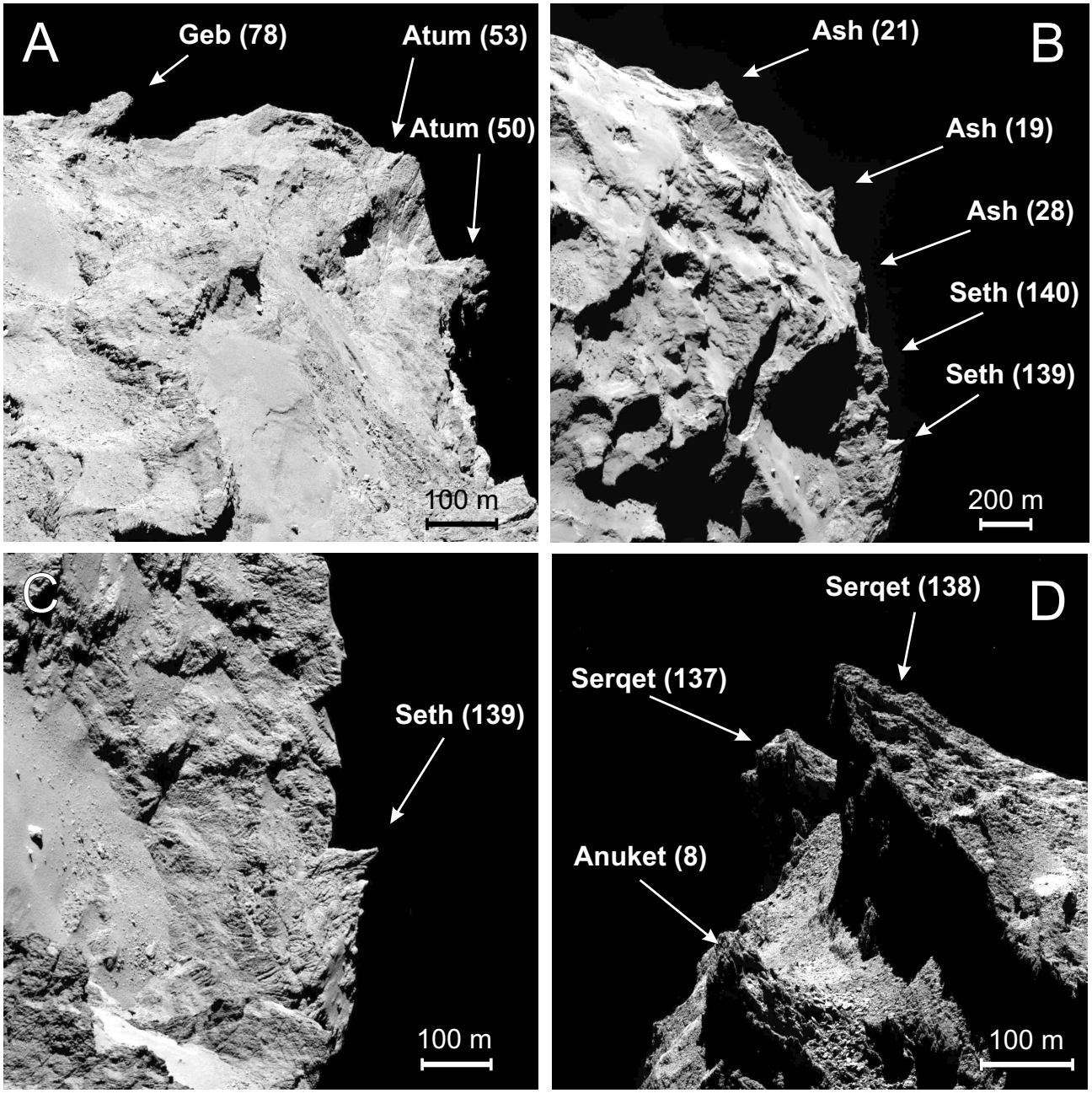

Figure 1. Examples of texture and morphology of pinnacles on OSIRIS images (N20160617T015626743ID30F22, N20150320T021247587ID30F22, N20160608T142857716ID30F22 and N20141006T004850558ID30F22). One can see boulders that are clearly distinguishable at the base of the pinnacles (Anuket 8 and Geb 78 in panels D and A). Sometimes, the base is covered with fine material (the Ash region in panel B). The examples of the knobs' texture can be found in panel D.

54 rounded pinnacles are identified on the nucleus surface of comet 67P (Table 1 and Table A1). They have planimetrically isometric shapes and heights varying from 9 to 93 meters (Table 1). The mean height is 31 m and its standard deviation is 20 m. This obviously indicates large variations of heights of the studied objects. The corresponding histogram is shown in the left part of the top row of Fig. 5. The four highest pinnacles have heights about three times larger than the mean value. All of them are located on the big lobe of the comet and have signatures of side erosion, which probably led to the formation of steep cliffs.

Distributions of small (d) and large (D) baselines are shown in the middle and right parts of the top row of the same figure. It is clearly seen that these distributions are similar to each other, and less flattened than the height distribution. One can see pronounced maxima in the region of 40 - 80 meters for d and in the region of 40 - 120 for D, respectively. At the same time, the full range of values is

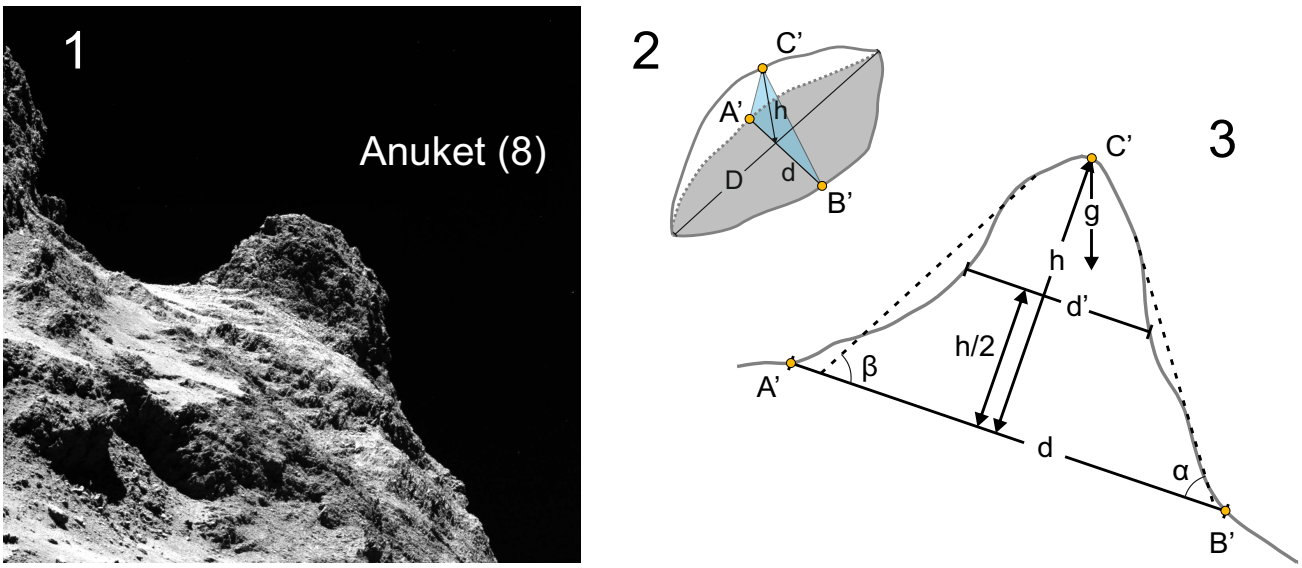

Figure 2. The Anuket 8 pinnacle (see Table A1 in Supplementary materials) located in the Anuket region (OSIRIS image N20141014T202103305ID30F22) is shown in panel 1. Sketches of a planimetric view and a side view including definitions of measured parameters are shown in panels 2 and 3, correspondingly. In the OSIRIS image, the top of the pinnacle is not visible due to the shooting direction from bottom to top. The knobby surface texture is clearly visible.

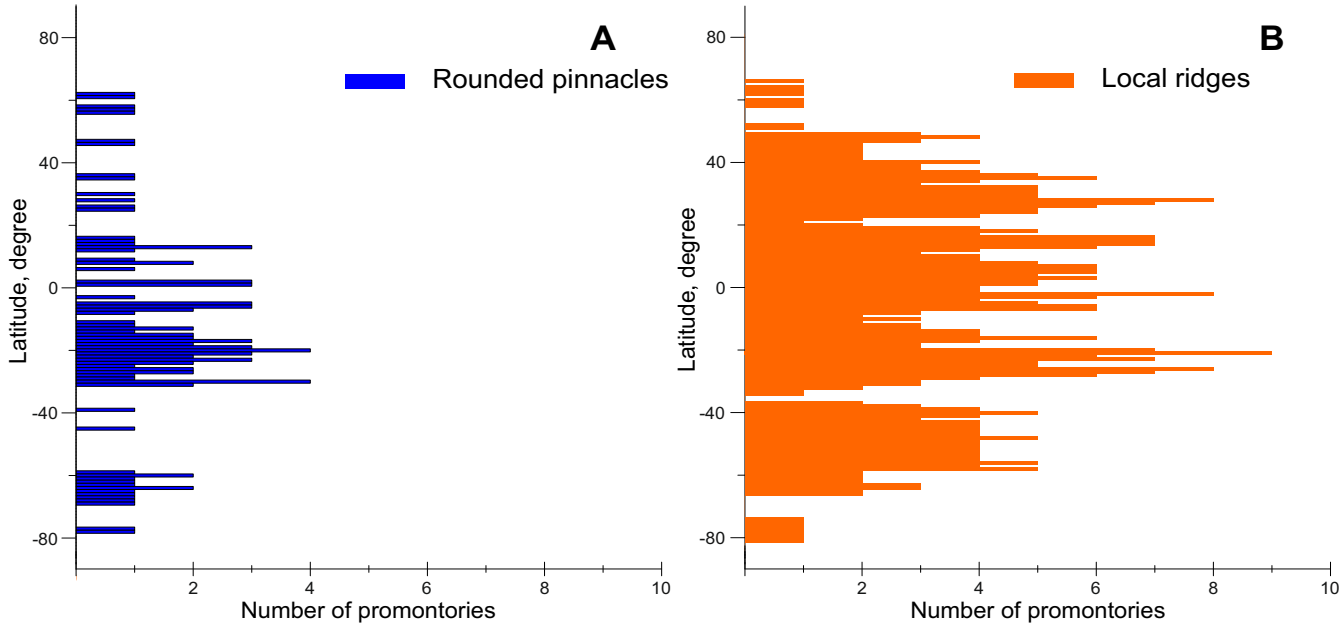

Figure 3. Distribution of local promontories depending on the feature latitude. Panel A: rounded pinnacles, panel B: local ridges.

rather extended: for example, d varies from 18 to 270 m and its mean value is about 80 m.

In the bottom row of the Fig. 5, we plot histograms for the ratios of the measured characteristics. The distribution presented in the left column (d/D) simply illustrates the absence of a prominent maximum. Distributions for (h/d) (middle column) and (h/D) (right column) have prominent maxima, with a mean value of about 0.4 and a standard deviation of 0.16, similar to a Maxwell-Boltzmann distribution. The distribution of the ratio of the half height of a pinnacle ($h/2$) to its small section (d') looks similar with values for mean and standard deviation 0.34 and 0.17, respectively. This similarity allows us to assume that the pinnacle shape does not substantially change with height and that our rounded pinnacles are self-similar figures. As it was mentioned in the previous section of the paper all morpho-

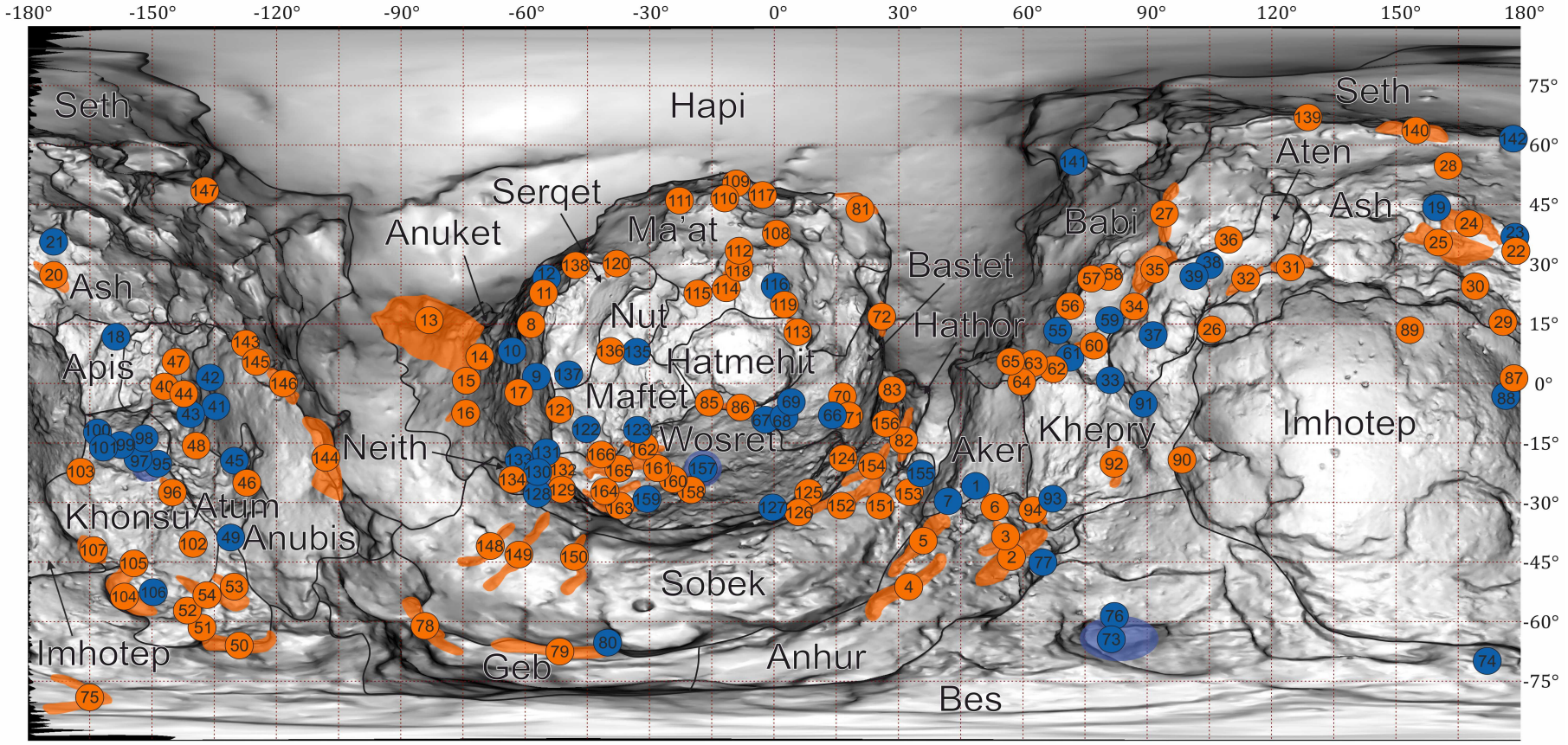

Figure 4. Map of rounded pinnacles (blue) and local ridges (orange) in equidistant cylindrical projection. Semi-transparent color shown real location of pinnacles on the map. For each promontory, the given assigned number is given. Metrical and statistical parameters shown in (Table A1).

Table 1. Statistical parameters of pinnacles in their morphological groups. N - number; $\overline{x}$ - mean; σ - standard deviation; R - range: minimum and maximum; Φ tilt angle - mean pinnacles' inclination to local gravity; α and β - mean slope inclination for flatter and steeper side.

Feature type	Location	N	Smaller base line d, m			Longer base line D, m			Height h, m			h/d		(h/2)/d'		Φ, deg	α & β , deg
			$\overline{x}$	σ	R, m	$\overline{x}$	σ	R, m	$\overline{x}$	σ	R, m	$\overline{x}$	σ	$\overline{x}$	σ	$\overline{x}$	$\overline{x}$
Rounded pinnacles	North	16	71	34	34 - 148	87	38	45 - 177	32	19	13 - 88	0.46	0.19	0.35	0.15	64	53 & 77
	South	38	83	56	29 - 269	99	68	33 - 349	34	22	10 - 93	0.42	0.15	0.36	0.15	57	36 & 71
	Total	**54**	**80**	**51**	**29 - 269**	**95**	**61**	**33 - 349**	**33**	**21**	**10 - 93**	**0.43**	**0.16**	**0.35**	**0.15**	**59**	**41 &73**
Local ridges	North	50	63	47	22 - 279	199	141	43 - 605	37	22	10 - 104	0.66	0.36	0.49	0.22	54	54 & 80
	South	62	75	52	23 - 378	268	153	53 - 736	33	23	9 - 137	0.47	0.24	0.39	0.2	54	44 & 69
	Total	**112**	**70**	**50**	**22 - 378**	**237**	**151**	**43 - 736**	**35**	**23**	**9 - 137**	**0.56**	**0.31**	**0.44**	**0.22**	**54**	**49 & 74**

metric parameters of the rounded pinnacles do not show statistically significant differences (at 95% confidence level) between north, south and the total nucleus surface.

The assumption that rounded pinnacles are self-similar, is supported by a simple analysis of the data presented in Fig. 6. Here show all pinnacles in the coordinates of the height h and smaller baseline d. If we exclude two objects having an "unusually" large height, then all remaining demonstrate a clear self-similarity: the cross-section d increases evenly as the height increases.

Local ridges

We identify 112 elongated pinnacles (local ridges) on the nucleus surface (Table 1 and Table A1). Their height varies from 9 m to 137 m with a mean value of 36 m and a standard deviation of 24 m (Table 1). The range of height variation differs little from the range of rounded pinnacles. At the same time, the histogram of the height distribution (Fig. 7) is somewhat different from that shown in Fig. 6. The number of small ridges (<20m) is noticeably larger, a well-marked maximum lies in a narrow height range 20m < h <40m, there is no peak in the region of maximum values of height, i.e. there are no unusually high ridges. The distributions of the small baseline (d) and the big baseline (D) are shown in the middle and in the right parts of the top row, respectively. The values of (d) vary from 22 to 380 meters and have a mean value of 71 m. This value is slightly smaller than the mean for rounded pinnacles. Structures that have heights comparable to those of rounded pinnacles are characterized by a markedly greater maximum extent. As in the case of rounded pinnacles, a prominent maximum is observed in the same range of values 40m < d <80m. There are slightly more pinnacles with small values of (d). But the distribution of the large baseline (D) differs more markedly: instead of a narrow maximum, we observe a broader distribution, which is more like a distribution of heights. Values of (D) vary from 43 to 736 meters with a mean value of 238 and a standard deviation of 151. Heights of local ridges differ little from the heights of rounded pinnacles.

The features noted above are even more pronounced when we analyze the distribution of ratios of model characteristics. They are shown in the bottom row of the Fig. 7. Looking at the statistics for rounded pinnacles, we observe a constant flat distribution of the (d/D) ratio in the interval 0.7 - 1. For the ratio we see clearly the predominance of small values: for a significant part of the local ridges, this ratio is less than a half of what it should be according to their type. Minor broadening of the distributions for (h) and (d) leads to a more pronounced broadening of the distribution for their ratio (middle column). But it is more interesting to compare this distribution with the distribution of the ratio of half height ($h/2$) to minor baseline (d') (right column). For rounded pinnacles this distribution is similar, which allowed us to assume self-similarity of these structures. Now it looks different: the distributions presented are clearly different, that is, our local ridges are not self-similar. This conclusion confirms the analysis of the data shown in Fig. 8 (its structure is similar to Fig. 6). The mean value of the ratio (h/d) is about 0.55, whereas for the ratio ($h/2$) to (d') the mean value is about 0.43. One can also note a higher clustering (compactization of the distribution) of local ridges for small values of (h) and (d), and a markedly greater dispersion for medium and large values of these model characteristics in comparison with the data obtained for round pinnacles (Fig. 8).

3 DISCUSSION

In this work we follow the assumption of Brownlee et al. (2004) that pinnacles are local topographic promontories, formed by sublimational loss of the surrounding surface material and their presence is an indication of inhomogeneities in the comet nucleus material. In this case the inhomogeneities reflect varying resistance to erosion. On the cometary surface erosion can be caused by various processes leading to destruction of the consolidated material (for example, thermal stresses, resulting in the formation of cracks, or dynamic stresses due to the rotation of the nucleus, or, finally, sublimation of volatiles accompanied by the removal of material). Contribution and importance of different processes require detailed analysis which we will perform in the next work using computer models. In the current work, we merely assume that the inhomogeneous sublimational erosion is the most reasonable process of pinnacle formation. If pinnacles formed as erosional remnants, their maximum height is a measure of minimum thickness of the lost eroded layer. This allows us to estimate the degree of change of the cometary nucleus during the time it is in the inner region of the solar system.

The 166 topographic promontories (pinnacles) were subdivided into two classes: 1) rounded pinnacles with d/D > 0.7, their total number is 54, and 2) local ridges with

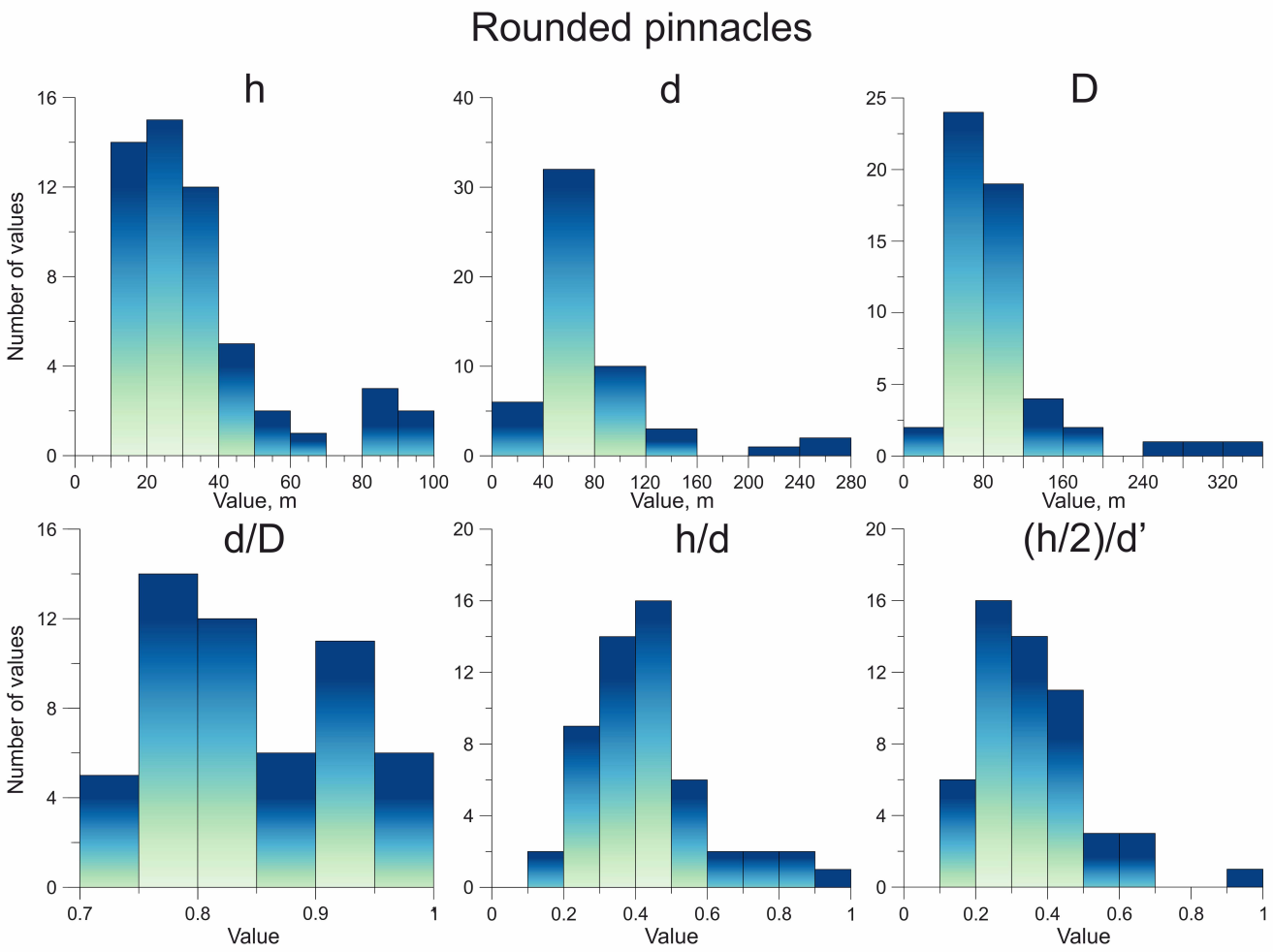

Figure 5. Histograms of morphometric parameters of the rounded pinnacles.

$d/D < 0.7$, their total number is 112. In the southern hemisphere, the numbers of both round pinnacles (38) and local ridges (62) are larger than in the northern hemisphere (16 and 50, correspondingly). These differences seem significant and possibly indicate the higher effectiveness of the pinnacle formation in the southern hemisphere. Orbit and rotation parameters of the 67P entail that its north hemisphere sees significantly smaller amount of sublimation than its southern counterpart. The southern surface displays consolidated nucleus material and is outcropped while in the north the surface is widely covered by loose material supposedly transported through the coma from the south (Keller et al. 2015, 2017). So, one may suggest that the observed difference in the number of promontories in the north and in the south is the result of the mentioned differences in illumination and presence/absence of the loose surface material. But at the same time, it was shown above that the mean values of the most of considered parameters, including the height (h), show no statistically reliable difference at the 95% confidence level between the northern and southern hemispheres. This output does not support speculation about the higher effectiveness of the promontory formation in the south comparing to the north. We hope to resolve this contradiction in future studies.

Among the studied 166 pinnacles of the 67P nucleus there are several round pinnacles and local ridges having highs between ~90 m and ~140 m. Within the assumptions made above these values can be considered as a minimum thickness of the eroded layer. It was also noted above that the heights of pinnacles in the north and in the south do not differ at the 95% confidence level. So, probably we may say that nucleus of the 67P comet had lost as minimum the 100 - 150 m thick layer of its material. It was shown (Keller et al. 2015) that at the present orbit the 67P nucleus loses a surface layer about a few meters thick per orbit. Thus, to grow such high formations about 50 orbits would be required. We should note that this estimate gives us only a minimum guideline, because the recent studies have not provided firm evidence of this estimate for the rate of erosion. It should also be remembered that orbits of the comets of the Jupiter family, to which comet 67P belongs, are rather changeable. Thus, the current orbit was formed most likely after 1959 (Ip et al. 2016) (i.e. ten orbits ago). Presently the erosion rate due to sublimation is about 4 times higher on the south than on the north Keller et al. (2015). The fact that the

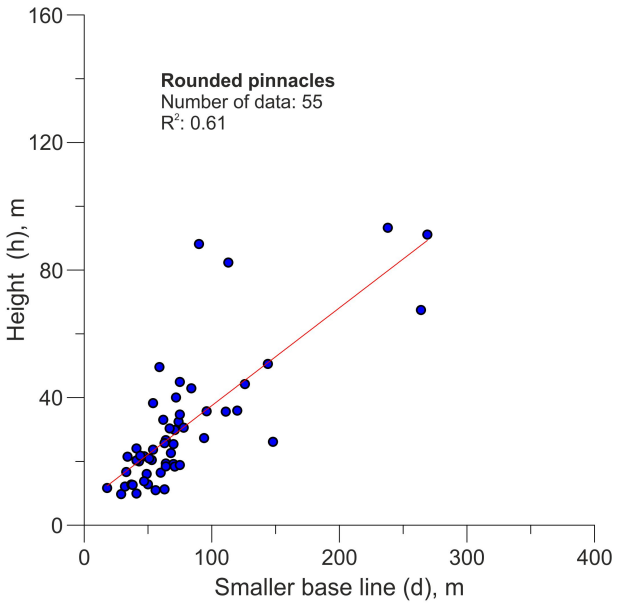

Figure 6. Ratio of height h to smaller base line d for rounded pinnacles.

pinnacles show about the same high on both hemispheres indicate that the orbit geometry preferring sublimation on the south could not have lasted long. In this connection, an interesting problem arises: can we see traces of past epochs in the structure of pinnacles (when the parameters of the orbit were, possibly, quite different). This problem requires attention and careful analysis.

Presence of 166 pinnacles having about 100 to 250 m in their planimetric baselines (for rounded pinnacles and local ridges) on the 67P nucleus provides information of lateral inhomogeneity of its material. Total surface area of the 67P nucleus surface is ~5 x 10^7 m^2 (Keller et al. 2015), so on average one pinnacle of the mentioned size is present at each ~3 x 10^5 m^2 , that is ~550 x 550 m. As was shown (Fig. 4) that the distribution of pinnacles over the entire surface is fairly uniform. At the same time, there are significant areas where we did not find pinnacles. Today we don't understand, what caused this. It is not clear which part of the pinnacle base is composed of the erosion-resistant material and which just results from the downslope movement of material.

The number of round pinnacles is smaller than the number of local ridges, this is observed for the northern and the southern hemispheres. This obviously means that the suggested inhomogeneities in the erosion of nucleus material are more often elongated than equidimensional. For the total sample of the studied promontories the mean ratio of the shorter base to the longer base is ~0.88 for round pinnacles and ~0.36 for local ridges (Table 1). Interesting is that the class of small promontories, so-called knobs, is characterized as rather planimetrically equidimentional (Sierks et al. 2015; Davidsson et al. 2016; Basilevsky et al. 2017b). This may be important for the processes of formation of the cometary material. As we noted above, regional ridges, mentioned by El-Maarry et al. (2016) represent the higher level of the surface heterogeneities. On the surface of comet 67P, we identified five formations of this type (Fig. A1 in the Supplementary materials).

The mean values of ratios of the measured pinnacle heights (h) to their smaller baselines (d) vary around 0.5. This ratio measured at half height can be considered a good indicator for the evolutionary growth of pinnacles. If the inhomogeneities of the pinnacle-forming nucleus material is very resistant to the sublimational erosion, pinnacles should be tall and narrow columns. If the resistance of the inhomogeneities is only slightly higher than that of the surrounding material, pinnacles should be low and gentle-sloping hills. The mentioned h/d values close to 0.5 suggest a moderate difference in resistance to erosion. A more quantitative estimate remains to be determined in future studies.

We calculated the inclinations of pinnacles and their slopes relative to the local gravity geometry. The mean slope inclination of rounded pinnacles is about 58(±24) and of local ridges 61(±21). The mean deviation from the plumb line (marked as g, on the Fig. 2) is ~34with standard deviation ±20and statistical dispersion near 90. The mean inclination and large dispersion show that the three-dimensional orientation of pinnacles on the surface are only weakly dependent on gravity. This is probably due to the very low gravity on the surface of 67P (~10^{-4} of the Earth g).

Positive topographical structures were observed on nuclei of previously explored comets (Fig. 9), such as comets 1P/Halley, 81P/Wild 2, 19P/Borrelly, 9P/Tempel 1, 103P/Hartley 2. As it mentioned previously, availability of pinnacles on the surface of 81P/Wild 2 were discussed in Brownlee et al. (2004), Basilevsky & Keller (2006) and Cheng et al. (2013) papers. For the surface of other nuclei rough terrains, large-scale ridges and hills were discussed but not specify as pinnacles. On comet 1P/Halley morphological formations like mountains, chains of hills and ridges were detected for the first time by Keller et al. (1988, 2004). The best resolution of the analyzed images was ~50 m/pix. The authors identified a chain of hills with a typical scale length of 0.5 - 1 km. On comet 19P/Borrelly, series of ridges of 1 - 2 km in length and about 200 m in high were found (Britt et al. 2004). They were oriented normally to the long axis of the comet and the authors speculated that their presence could be an indication of at least one episode of compressional stress of the nucleus (Britt et al. 2004). The resolution of the images was around ~50 m/pix. Extended ridges were found on the comet 9P/Tempel 1 (Belton et al. 2013; Thomas et al. 2013). The best resolution of the images was around 13 m/px. The images with approximately the same resolution (~12 m/pix) of 103P/Hartley 2 nucleus allow to found parallel ridges (Syal et al. 2013) oriented normally to the long axis of the comet, as it mentioned for 19P nucleus. Different types of positive topographical features also were found (A'Hearn et al. 2011; Thomas et al. 2013). Near the neck of the bilobate shaped Hartley 2, the features, which look like ridges on the Borrelly nucleus, can also be identified. These barely-recognizable ridges were oriented normal to the long axis of comet. On the surface of comet Hartley 2 separate positive topographical features, few tens of meters in diameter, described by A'Hearn et al. (2011) and Pajola et al. (2016), look like ridges on comet Borrelly (Fig. 9). All these positive features are probably kindred to pinnacles of comet Churyumov-Gerasimenko suggesting

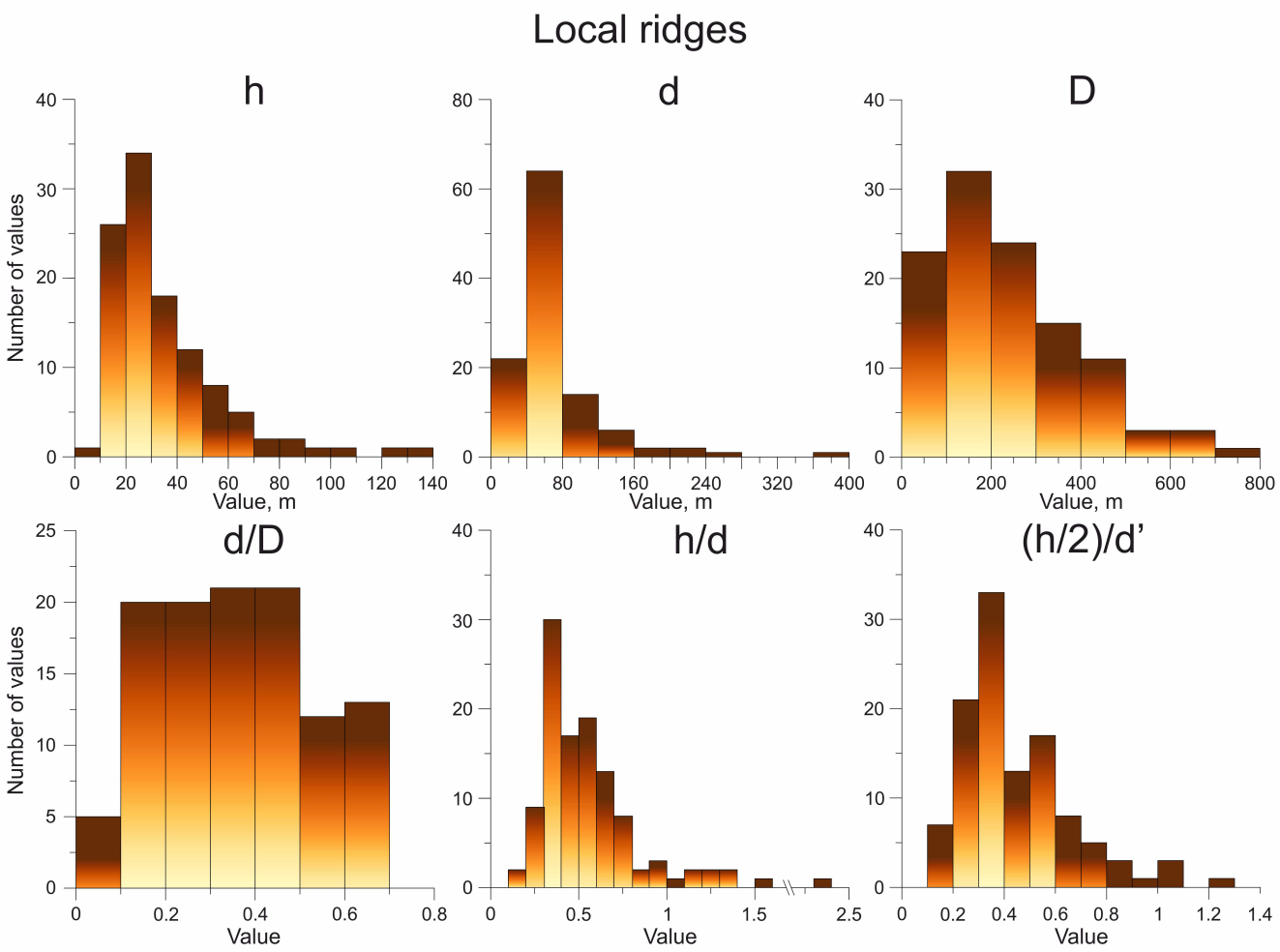

Figure 7. Histograms, based on metric data of local ridges.

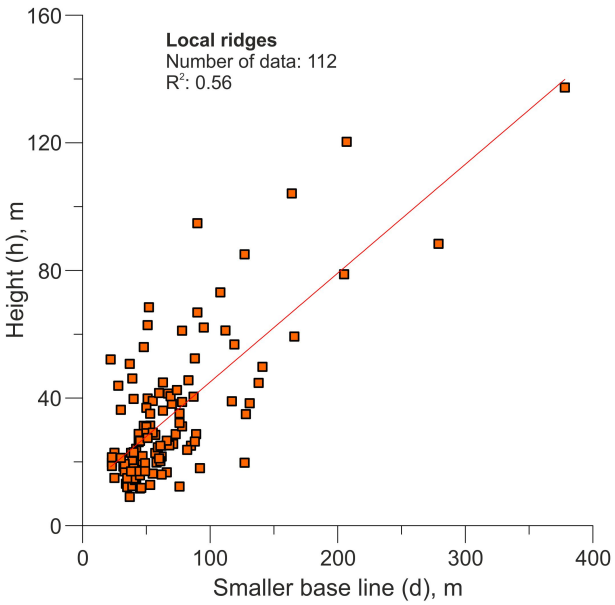

Figure 8. Ratio of height h to smaller base line d for local ridges.

that areally varying surface erosion is a typical process on comet nuclei.

We note that one of the possible mechanisms of inner inhomogeneity formation and bi-lobate form can be the collision of two bodies (Massironi et al. 2015; Schwartz et al. 2018) or accretion processes (Davidsson et al. 2016). Modeling of these processes is performed by Jutzi & Benz (2017). As a result, regional ridges or depressions, oriented normally to the long axis of the comet, as it assumed for comet Borrelly (Britt et al. 2004) and found on the surface of comet Hartley 2, can be formed. In paper Pajola et al. (2019), the distribution of boulders in the Hapi region, located between two main bodies, is considered. The presence of aligned "ridge" made of boulder-like features in the centerline of the region, is associated with the destruction of a layer of bigger comet lobe (Pajola et al. 2019). Origin of boulder-like features as a destroyed layer is possible, however, it needs to remember, that the Hapi region is subject to complicated denudation and accumulation processes. Active accumulation of material probably occurs during the redeposit of loose material from south to north (Keller et al. 2017). The probable destruction of the Seth and the Hathor regions (Pajola et al. 2019) can also lead to an accumulation of ma-

terial in Hapi region. Loss of material occurs during activity and jets, coming from Hapi (Sierks et al. 2015). Therefore, aligned "ridge" made of boulders-like features in Hapi can be either destroyed analog of ridges in the southern regions like Sobek and Neith or can be the destroyed material of the Seth or/and the Hathor regions. Thus, these boulders are hard to relate to the ridges or product of the destroyed region and they are not considered as pinnacles in this work.

From the beginning of the discovery of positive topographical features on cometary nuclei (in this paper only part of them - pinnacles, were described), two main scenarios (and many options between them) are discussed: these formations are related to the activity of the comet, that is, are evolutionary; or they reflect the formation of a comet, that is, they are pristine (possibly partly modified by activity). Brownlee et al. (2004) following the first hypothesis speculates about two possible scenarios of origin: they are formed as more stable erosional remnants, created by loss of weaker surrounding material, or they formed by erosion of mesas and wall collapse. Basilevsky & Keller (2006) and Cheng et al. (2013) also connected the pinnacle formation with surface erosion and degradation of surrounding material. This idea seems all the more attractive because formations similar to cometary pinnacles have recently been discovered on other icy bodies of the solar system (see e.g., Howard & Moore 2008; Moore et al. 2017).

4 CONCLUSIONS

High-resolution imaging of nucleus of comet 67P Churyumov-Gerasimenko allowed us to identify and map 166 local topographic promontories, so-called pinnacles, whose characteristics provide some information on the structure of the nucleus material and on the scale of the sublimational erosion.

In relation of their planimetric outlines pinnacles were subdivided into round ones and local ridges. The latter dominate in number over the first ones. This implies that a significant part of the suggested inhomogeneities of the nucleus material is not geometrically equidimensional but elongated.

The number of pinnacles on the southern part of the nucleusis is larger than that on the north. This could indicate a different effectiveness of pinnacle formation.This suggestion, however, seems to contradict the observation that the pinnacles heights on the south and north are statistically similar. Thus, further analysis of this issue is necessary.

The maximum heights of the pinnacles (90 - 140 m) requires that the nucleus of 67P erosionally lost at least a comparable thick layer of its material on both hemispheres, i. e. overall. About 50 approaches to the Sun are required for this, however, not on orbits similar to the present one. Presently the sublimation on the hemispheres is too different.

The relative heights of the pinnacles (mean h/d ~0.5) suggest moderate differences of the erosion resistance between the pinnacle-forming material and its surrounding. Looking at images of other comet nuclei (which are of much lower resolution than those of 67P nucleus) suggests that pinnacle covered land forms are typical for comets.

ACKNOWLEDGEMENTS

SK supported by Deutscher Akademischer Austauschdienst. Work of SK and AB was partly supported by grant 0137-2018-0038, Program I.28 by Presidium of Russian Academy of Sciences. Yu.S. thanks the Deutsche Forschungsgemeinschaft (DFG) for support under grant SK 264/2-1. The authors appreciate the assistance of D. Brazier.

REFERENCES

A'Hearn M. F. et al., 2011, Science, 332, 1396
Attree N. et al., 2018, A&A, 611, A33
Basilevsky A. T., Keller H. U., 2006, Planet. Space Sci., 54, 808
Basilevsky A. T., Krasilnikov S. S., Mall U., Hviid S. F., Skorov Yu. V., Keller H. U., 2017a, Planet. Space Sci., 140, 80
Basilevsky A. T., Mall U., Keller H. U., Skorov Yu. V., Hviid S. F., Mottola S., Krasilnikov S. S., Dabrowski B., 2017b, Planet. Space Sci., 137, 1
Belton M. J. S. et al., 2013, Icarus, 222, 477
Bibring J.-P. et al., 2015, Science, 349, 671
Britt D. T. et al., 2004, Icarus, 167, 45
Brownlee D. E. et al., 2004, Science, 304, 1764
Cheng A. F., Lisse C. M., A'Hearn M., 2013, Icarus, 222, 808
Davidsson B. J. R. et al., 2016, A&A, 592, A63
El-Maarry M. R. et al., 2015a, A&A, 583, A26
El-Maarry M. R. et al., 2015b, Geophys. Res. Let., 42, 5170
El-Maarry M. R. et al., 2016, A&A, 593, A110
Geiger G., Barthelemy M., 2015, ESA PSA, NASA PDS
Giacomini L. et al., 2016, MNRAS, 462, 352
Howard A. D., Moore J. M., 2008, Geophys. Res. Let., 35, L03203
Ip W.-H. et al., 2016, A&A, 591, A132
Jutzi M., Benz W., 2017, A&A 597, A61
Keller H. U. et al., 2004, Univ. of Arizona Press, 211
Keller H. U. et al., 2007, Space Sci. Rev. 128, 433
Keller H. U. et al., 2015, A&A, 583, A34
Keller H. U. et al., 2017, MNRAS, 469, 357
Keller H. U., Kramm R., Thomas N., 1988, Nature, 331, 227
Lee J.-C. et al., 2016, MNRAS, 462, 573
Lipar M., Webb J. A., 2015, Earth-Sci. Rev., 140, 182
Massironi M. et al., 2015, Nature, 526, 402
Moore J. M. et al., 2017, Icarus, 287, 45
Mottola S. et al., 2015, Science, 349, 6247
Pajola M. et al., 2016, A&A, 585, A85
Pajola M. et al., 2019, MNRAS 485, 2139
Preusker F. et al., 2017, A&A, 607, L1
Schwartz S. R. et al., 2018, Nature, 2, 379
Sierks H. et al., 2015, Science 347, aaa1044
Syal B. M., Schultz P. H., Sunshine J. M., A'Hearn M.F., Farnham T. L., Dearborn D. S. P., 2013, Icarus, 222, 610
Thomas P. et al., 2013, Icarus, 222, 453

APPENDIX A: SUPPLEMENTARY MATERIAL

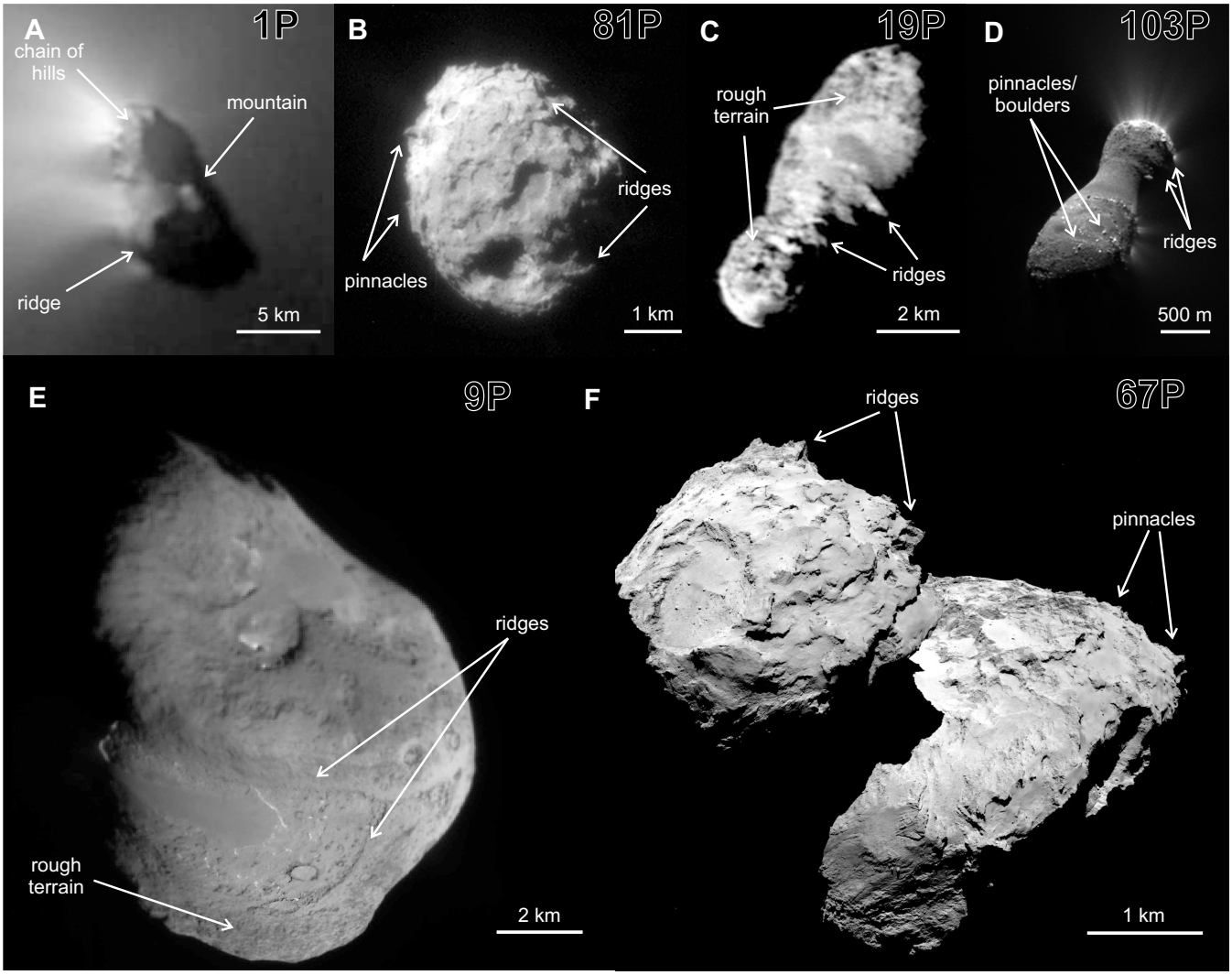

Figure 9. Positive topographical features, which can be interpreted as pinnacles and ridges on the comet nuclei: A - chain of hills, ridge and mountain (Keller et al. 1988, 2004) on comet 1P/Halley; B - pinnacles (Brownlee et al. 2004) and possible ridges on the comet 81P/Wild 2; C - ridges and rough territory (Britt et al. 2004) on comet 19P/Borrelly; D - ridges (Syal et al. 2013) and potential pinnacles/boulders on the surface of comet 103P/Hartley 2 (A'Hearn et al. 2011; Pajola et al. 2016); E - potential ridges and rough territory (Belton et al. 2013; Thomas et al. 2013) on comet 9P/Tempel 1; F - pinnacles and ridges (Basilevsky et al. 2017a) on comet 67P/Churyumov-Gerasimenko.

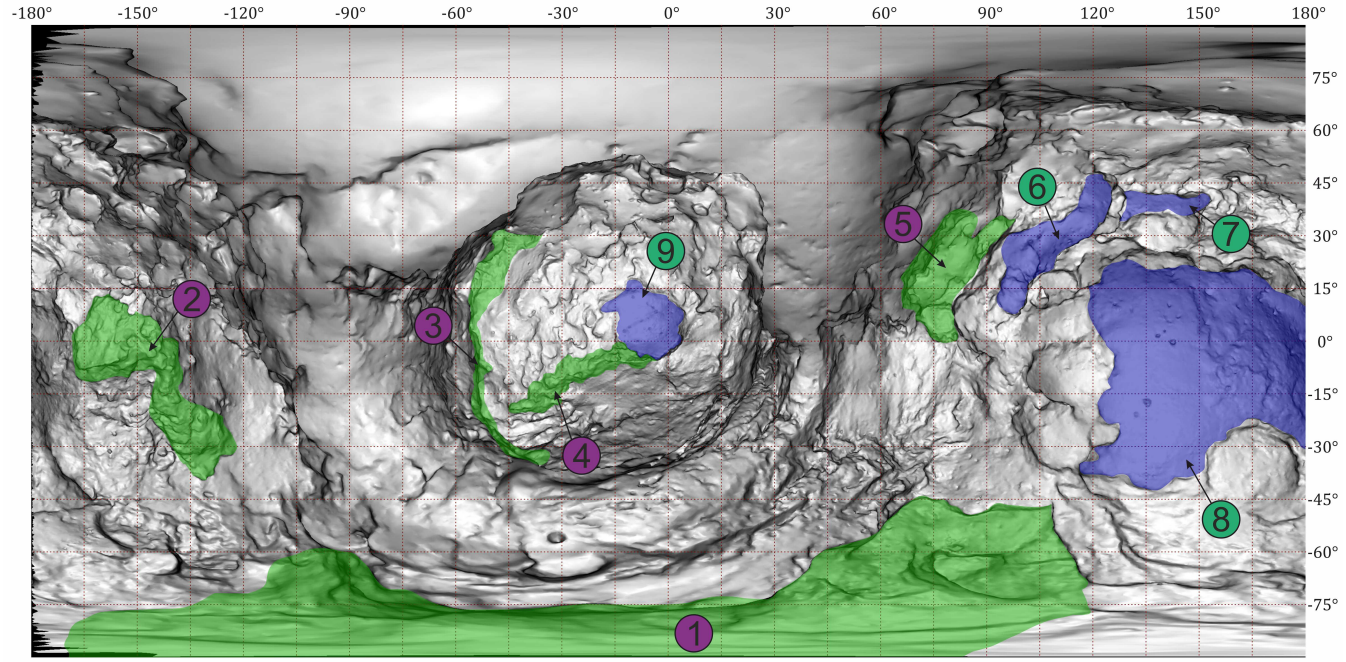

Figure A1. Regional ridges (1 - 5), prolonged (6 and 7) and merged (8 and 9) regional depressions.

Table A1. Metrical parameters for pinnacles.

	Region	Type	Smaller direction (d)	Bigger direction (D)	d/D	Height (h)	h/d	(h/2)/d'	Tiltangle, degree	Slopes angle, degree	Coordinates	
											Lat.	Lon.
1	Aker	rounded	29	38	0.76	10	0.34	0.38	55	22 & 49	-27.2	48.1
2	Anhur	ridges	117	673	0.17	39	0.33	0.30	58	31 & 62	-44.3	55.8
3	Anhur	ridges	34	230	0.15	13	0.39	0.36	77	36 & 48	-41.6	51.3
4	Anhur	ridges	32	440	0.07	19	0.58	0.45	63	60 & 81	-50.2	34.5
5	Anhur	ridges	44	492	0.09	29	0.65	0.62	80	64 & 66	-39.2	36
6	Anhur	ridges	78	310	0.25	39	0.50	0.32	82	54 & 80	-30.6	45.9
7	Anhur	rounded	75	91	0.82	45	0.60	0.57	55	56 & 70	-30.9	41.1
8	Anuket	ridges	121	178	0.68	87	0.72	0.75	35	51 & 65	15.3	-60.3
9	Anuket	rounded	56	65	0.86	11	0.20	0.16	13	24 & 58	9.3	-56.2
10	Anuket	rounded	33	33	1.00	12	0.37	0.29	13	23 & 72	8.5	-63.6
11	Anuket	ridges	53	254	0.21	13	0.24	0.21	34	28 & 37	23.5	-54.9
12	Anuket	rounded	41	53	0.77	10	0.24	0.23	13	28 & 37	26	-55.2
13	Anuket	ridges	378	640	0.59	137	0.36	0.25	66	42 & 77	16.8	-76.2
14	Anuket	ridges	62	180	0.34	25	0.40	0.41	32	42 & 58	7.8	-66.4
15	Anuket	ridges	35	109	0.32	12	0.34	0.34	67	36 & 88	0.7	-75.8
16	Anuket	ridges	39	75	0.52	12	0.32	0.31	-2	40 & 73	-7.2	-73
17	Anuket	ridges	28	84	0.33	44	1.57	1.28	33	44 & 63	-1.8	-63
18	Apis	rounded	50	54	0.93	16	0.32	0.25	89	33 & 36	12.4	-158.6
19	Ash	rounded	90	112	0.80	88	0.98	0.62	64	79 & 90	46.4	160.4
20	Ash	ridges	39	130	0.30	21	0.53	0.54	57	77 & 84	28	-176
21	Ash	rounded	34	48	0.71	22	0.63	0.50	80	51 & 82	35.9	-174.9
22	Ash	ridges	33	53	0.62	17	0.52	0.58	60	52 & 62	36.1	178.9
23	Ash	rounded	43	45	0.96	20	0.47	0.41	58	63 & 91	37.2	178.5
24	Ash	ridges	205	605	0.34	79	0.38	0.24	62	46 & 53	40.3	170
25	Ash	ridges	279	565	0.49	88	0.32	0.18	73	69 & 77	33.9	162.7
26	Ash	ridges	51	98	0.52	40	0.78	0.46	87	63 & 92	13.8	106.2
27	Ash	ridges	25	412	0.06	23	0.91	0.66	89	71 & 85	46	94.5
28	Ash	ridges	87	490	0.18	40	0.46	0.31	31	36 & 96	49	176.3
29	Ash	ridges	88	205	0.43	52	0.60	0.51	62	41 & 85	14.3	175.6
30	Ash	ridges	73	106	0.69	29	0.39	0.30	54	60 & 82	23.5	168.6
31	Aten	ridges	112	178	0.63	61	0.55	0.31	56	70 & 101	30.3	122.5
32	Aten	ridges	48	157	0.31	56	1.17	0.81	53	76 & 77	26	112.1
33	Aten	rounded	62	87	0.71	33	0.53	0.39	45	67 & 73	0.6	81.1
34	Aten	ridges	41	172	0.24	14	0.35	0.21	41	66 & 82	17.1	85.2
35	Aten	ridges	164	366	0.45	104	0.64	0.34	48	74 & 95	31.8	91.9
36	Aten	ridges	45	93	0.48	12	0.26	0.24	50	32 & 87	34.9	111.2

	Region	Type	Smaller direction (d)	Bigger direction (D)	d/D	Height (h)	h/d	(h/2)/d'	Tiltangle, degree	Slopes angle, degree	Coordinates	
											Lat.	Lon.
37	Aten	ridges	50	90	0.56	16	0.31	0.23	38	60 & 91	13.6	91
38	Aten	ridges	22	52	0.42	10	0.46	0.77	42	61 & 84	29.6	104.3
39	Aten	rounded	35	48	0.73	16	0.45	0.42	52	62 & 57	28.3	102.2
40	Atum	ridges	47	71	0.66	20	0.43	0.38	67	38 & 53	0.6	-147.6
41	Atum	rounded	100	120	0.83	49	0.49	0.47	33	33 & 40	-4.6	-134.1
42	Atum	rounded	60	72	0.83	16	0.27	0.23	43	26 & 48	1.2	-135.4
43	Atum	rounded	75	76	0.99	31	0.42	0.30	47	48 & 86	-7.5	-140.1
44	Atum	ridges	95	150	0.63	32	0.34	0.25	56	41 & 56	-2	-145
45	Atum	rounded	64	85	0.75	27	0.42	0.46	56	44 & 80	-20.1	-128.7
46	Atum	ridges	71	215	0.33	26	0.36	0.30	35	60 & 63	-26.6	-127.2
47	Atum	ridges	58	255	0.23	20	0.34	0.35	19	17 & 126	-2.6	-145.8
48	Atum	ridges	72	250	0.29	28	0.38	0.25	67	44 & 68	-16	-139
49	Atum	rounded	47	50	0.94	22	0.46	0.47	23	15 & 88	-39.4	-130.7
50	Atum	ridges	42	170	0.25	24	0.57	0.59	42	52 & 65	-64.9	-124.2
51	Atum	ridges	50	260	0.19	31	0.62	0.44	49	62 & 68	-56.3	-139.5
52	Atum	ridges	68	271	0.25	25	0.37	0.33	74	33 & 63	-58	-140
53	Atum	ridges	95	508	0.19	36	0.38	0.31	44	34 & 66	-50	-129
54	Atum	ridges	127	592	0.21	20	0.16	0.10	58	48 & 87	-52	-136
55	Babi	rounded	74	95	0.78	32	0.44	0.26	75	72 & 89	14.3	68.3
56	Babi	ridges	50	120	0.42	29	0.58	0.37	62	60 & 95	19.5	73.1
57	Babi	ridges	23	77	0.30	15	0.65	0.52	69	42 & 86	25.3	75.5
58	Babi	ridges	25	43	0.58	15	0.60	0.43	78	46 & 93	26.9	79.2
59	Babi	rounded	148	177	0.84	26	0.18	0.10	57	45 & 59	15.9	80.5
60	Babi	ridges	57	326	0.17	28	0.50	0.38	54	38 & 80	9.7	76.4
61	Babi	rounded	71	93	0.76	30	0.42	0.29	60	79 & 83	6.6	70.2
62	Babi	ridges	42	170	0.25	14	0.34	0.35	78	36 & 48	5	65.3
63	Babi	ridges	48	292	0.16	31	0.65	0.52	79	44 & 73	6.5	62.3
64	Babi	ridges	89	230	0.39	29	0.32	0.28	51	16 & 55	4.3	59.5
65	Babi	ridges	53	382	0.14	31	0.59	0.52	60	55 & 76	6.6	56.6
66	Bastet	rounded	84	104	0.81	43	0.51	0.44	78	29 & 67	-6.9	14.2
67	Bastet	rounded	63	68	0.93	29	0.45	0.34	66	22 & 47	-8.9	-2.8
68	Bastet	rounded	64	77	0.83	26	0.41	0.35	89	25 & 40	-6.9	0.3
69	Bastet	rounded	70	80	0.88	19	0.27	0.30	63	24 & 69	-5.8	3
70	Bastet	ridges	37	93	0.40	9	0.24	0.17	87	35 & 55	-3.3	16.7
71	Bastet	ridges	66	142	0.46	17	0.25	0.18	47	29 & 39	-10	17.2
72	Bastet	ridges	76	370	0.21	35	0.46	0.47	17	58 & 62	19.4	26.7
73	Bes	rounded	269	297	0.91	91	0.34	0.17	68	74 & 101	-65.2	86.3

	Region	Type	Smaller direction (d)	Bigger direction (D)	d/D	Height (h)	h/d	(h/2)/d'	Tiltangle, degree	Slopes angle, degree	Coordinates	
											Lat.	Lon.
74	Bes	rounded	113	149	0.76	82	0.73	0.55	52	55 & 81	-67.7	178.3
75	Bes	ridges	63	736	0.09	36	0.57	0.42	47	56 & 78	-78.6	-165
76	Bes	rounded	67	72	0.93	30	0.45	0.29	59	33 & 57	-58.9	80.9
77	Bes	rounded	41	44	0.93	24	0.59	0.40	64	55 & 80	-45.1	63.7
78	Geb	ridges	40	250	0.16	40	0.99	0.87	20	50 & 85	-56.4	-85.5
79	Geb	ridges	67	197	0.34	41	0.62	0.38	59	61 & 79	-67.8	-51.9
80	Geb	rounded	59	76	0.78	50	0.84	0.69	71	58 & 94	-63.3	-38.5
81	Hathor	ridges	52	238	0.22	68	1.32	0.73	31	71 & 94	47.7	20
82	Hathor	ridges	207	372	0.56	120	0.58	0.63	52	31 & 49	-14	30.7
83	Hathor	ridges	66	218	0.30	27	0.40	0.39	53	49 & 56	-0.3	33.3
84	Hathor	ridges	38	278	0.14	23	0.60	0.40	-2	78 & 80	11.7	25.7
85	Hatmehit	ridges	90	217	0.41	95	1.05	0.65	57	70 & 89	-15	-5.7
86	Hatmehit	ridges	108	328	0.33	73	0.68	0.57	58	64 & 78	-10.3	-5.8
87	Imhotep	ridges	61	139	0.44	21	0.35	0.31	72	37 & 49	-3.2	175.8
88	Imhotep	rounded	71	81	0.88	18	0.26	0.20	81	34 & 40	-0.9	177.9
89	Imhotep	ridges	46	77	0.60	12	0.26	0.25	72	29 & 46	13.3	152.4
90	Khepry	rounded	100	102	0.98	84	0.84	0.92	58	35 & 51	-19	99
91	Khepry	rounded	126	173	0.73	44	0.35	0.23	48	49 & 87	-4.1	88.1
92	Khepry	ridges	83	400	0.21	46	0.55	0.50	82	59 & 68	-18.2	81.9
93	Khepry	rounded	101	107	0.94	39	0.39	0.38	85	28 & 52	-28.7	66.2
94	Khepry	ridges	83	134	0.62	59	0.71	0.69	54	48 & 56	-30.6	61.2
95	Khonsu	rounded	238	274	0.87	93	0.39	0.29	80	44 & 58	-24.6	-150.6
96	Khonsu	ridges	131	239	0.55	38	0.29	0.20	84	32 & 61	-26.5	-147.7
97	Khonsu	rounded	63	67	0.94	11	0.18	0.14	35	39 & 64	-17.8	-152.9
98	Khonsu	rounded	111	112	0.99	36	0.32	0.28	85	36 & 45	-16.1	-152.2
99	Khonsu	rounded	94	124	0.76	27	0.29	0.21	74	28 & 103	-16.5	-158.1
100	Khonsu	rounded	64	74	0.86	18	0.29	0.25	88	33 & 76	-15.2	-160.5
101	Khonsu	rounded	53	68	0.78	20	0.39	0.34	59	36 & 101	-16.2	-161.2
102	Khonsu	ridges	82	128	0.64	24	0.29	0.19	77	46 & 67	-39.7	-141.9
103	Khonsu	ridges	62	145	0.43	22	0.35	0.25	64	39 & 52	-21.1	-168
104	Khonsu	ridges	76	178	0.43	12	0.16	0.11	68	42 & 46	-51.8	-157.6
105	Khonsu	ridges	61	117	0.52	20	0.33	0.31	86	32 & 37	-48	-149
106	Khonsu	rounded	47	52	0.90	22	0.47	0.46	59	28 & 82	-52.6	-149.5
107	Khonsu	ridges	141	237	0.59	50	0.35	0.28	46	37 & 79	-40.3	-165.8
108	Ma'at	ridges	63	196	0.32	45	0.71	0.63	20	38 & 90	40.5	1.5
109	Ma'at	ridges	48	77	0.62	39	0.80	0.62	35	62 & 71	52.8	-7.3
110	Ma'at	ridges	45	67	0.67	27	0.59	0.44	47	58 & 67	50	-10.2

	Region	Type	Smaller direction (d)	Bigger direction (D)	d/D	Height (h)	h/d	(h/2)/d'	Tiltangle, degree	Slopes angle, degree	Coordinates	
											Lat.	Lon.
111	Ma'at	ridges	45	97	0.46	27	0.59	0.36	47	60 & 75	46.8	-24
112	Ma'at	ridges	39	79	0.49	46	1.18	1.09	49	67 & 87	35.3	-7.8
113	Ma'at	ridges	138	309	0.45	45	0.32	0.26	73	53 & 85	13.9	6.9
114	Ma'at	ridges	23	89	0.26	19	0.81	0.73	64	67 & 70	26.6	-11.6
115	Ma'at	ridges	40	107	0.37	23	0.58	0.53	55	62 & 66	24.3	-17.9
116	Ma'at	rounded	75	84	0.89	38	0.51	0.35	87	68 & 72	23.5	0.2
117	Ma'at	ridges	30	85	0.35	21	0.71	0.50	8	40 & 99	50.4	-2.6
118	Ma'at	ridges	55	316	0.17	39	0.71	0.51	75	60 & 87	30.7	-6.9
119	Ma'at	ridges	47	200	0.24	22	0.46	0.42	55	43 & 100	19.8	1.8
120	Ma'at	ridges	50	97	0.52	37	0.74	0.57	30	37 & 82	31.5	-34.5
121	Maftet	ridges	57	84	0.68	23	0.40	0.27	44	57 & 70	-8.3	-50.6
122	Maftet	rounded	92	113	0.81	18	0.20	0.14	58	22 & 82	-11.5	-45
123	Maftet	rounded	144	157	0.92	59	0.41	0.25	74	38 & 95	-12.5	-34
124	Neith	ridges	78	244	0.32	31	0.40	0.31	33	45 & 56	-18.6	16.8
125	Neith	ridges	40	171	0.23	15	0.37	0.31	24	37 & 67	-23.8	9.5
126	Neith	ridges	23	53	0.43	21	0.93	0.64	68	71 & 96	-32.5	3.2
127	Neith	rounded	41	53	0.77	20	0.48	0.42	17	40 & 108	-33.7	-2.6
128	Neith	rounded	68	85	0.80	23	0.33	0.33	83	34 & 86	-28.7	-56
129	Neith	ridges	59	118	0.50	25	0.42	0.40	24	47 & 49	-26	-53.8
130	Neith	rounded	78	96	0.81	31	0.39	0.32	56	49 & 52	-27.2	-49.4
131	Neith	rounded	70	92	0.76	34	0.48	0.36	28	52 & 81	-24.9	-50.3
132	Neith	ridges	49	165	0.30	20	0.40	0.29	37	37 & 60	-18.3	-55.6
133	Neith	rounded	51	54	0.94	21	0.41	0.34	49	45 & 67	-21.8	-56.8
134	Neith	ridges	55	117	0.47	29	0.53	0.36	72	51 & 92	-19.7	-61
135	Nut	rounded	37	49	0.76	13	0.35	0.31	87	34 & 50	8.1	-33
136	Nut	ridges	45	105	0.43	16	0.35	0.29	70	33 & 50	8.2	-38.1
137	Serqet	rounded	38	54	0.70	13	0.33	0.23	65	26 & 105	2.4	-49.5
138	Serqet	ridges	60	166	0.36	42	0.69	0.54	56	58 & 78	31.6	-47.6
139	Seth	ridges	51	435	0.12	63	1.23	1.02	45	64 & 65	67.7	128.2
140	Seth	ridges	95	328	0.29	62	0.65	0.34	37	80 & 96	65.6	150.1
141	Seth	rounded	72	88	0.82	40	0.56	0.45	61	45 & 81	57.3	71.8
142	Seth	rounded	54	56	0.96	38	0.71	0.60	18	61 & 82	62.5	178.7
143	Seth	ridges	22	170	0.13	52	2.37	0.78	41	76 & 127	10.9	-128.8
144	Seth	ridges	53	360	0.15	35	0.66	0.50	35	59 & 98	-17.1	-108.3
145	Seth	ridges	30	61	0.49	36	1.21	0.96	55	57 & 82	5.5	-124.1
146	Seth	ridges	37	310	0.12	51	1.37	1.08	29	53 & 108	0.2	-118.1
147	Seth	ridges	40	60	0.67	18	0.45	0.46	27	34 & 52	48.8	-136.5

	Region	Type	Smaller direction (d)	Bigger direction (D)	d/D	Height (h)	h/d	(h/2)/d'	Tiltangle, degree	Slopes angle, degree	Coordinates	
											Lat.	Lon.
148	Sobek	ridges	44	470	0.09	17	0.39	0.34	49	39 & 85	-41	-69.6
149	Sobek	ridges	55	415	0.13	16	0.30	0.26	63	26 & 29	-38.3	-59.3
150	Sobek	ridges	35	310	0.11	15	0.43	0.29	58	70 & 82	-38.5	-48
151	Sobek	ridges	51	137	0.37	27	0.54	0.55	44	8 & 126	-31.8	25.3
152	Sobek	ridges	69	290	0.24	41	0.59	0.52	50	18 & 59	-29.5	19.7
153	Sobek	ridges	78	471	0.17	61	0.78	0.81	63	55 & 98	-27	33
154	Sobek	ridges	61	363	0.17	25	0.41	0.36	50	36 & 92	-21.4	24
155	Sobek	rounded	44	56	0.79	22	0.50	0.44	79	20 & 120	-21.7	34.1
156	Sobek	ridges	166	414	0.40	59	0.36	0.18	71	83 & 95	-10.1	28.6
157	Wosret	rounded	264	349	0.76	68	0.26	0.18	88	28 & 95	-24.8	-18.1
158	Wosret	ridges	119	205	0.58	57	0.48	0.34	63	36 & 50	-25.1	-24
159	Wosret	rounded	96	115	0.83	36	0.37	0.29	58	22 & 78	-30.1	-31.6
160	Wosret	ridges	49	177	0.28	17	0.35	0.38	59	37 & 54	-23.4	-28.7
161	Wosret	ridges	62	223	0.28	16	0.26	0.37	54	20 & 39	-22	-29.3
162	Wosret	ridges	60	136	0.44	21	0.35	0.29	72	48 & 47	-16.5	-30.5
163	Wosret	ridges	38	255	0.15	17	0.45	0.36	54	54 & 55	-28.9	-34.3
164	Wosret	ridges	128	423	0.30	35	0.27	0.20	69	35 & 59	-25.5	-36.7
165	Wosret	ridges	76	309	0.25	32	0.42	0.30	80	37 & 117	-22.9	-40.2
166	Wosret	ridges	74	250	0.30	43	0.57	0.40	70	48 & 95	-19.2	-44.2